27nJ, 114fs Pulses From an Environmentally Stable All-Normal All-PM Yb-Doped Fiber Laser Mode-Locked With a Nonlinear Amplifying Loop Mirror

Luqi Guo, Zebiao Gan, and Xiaoyan Liang

***Abstract*—We report on a self-starting mode-locked all-polarization-maintaining fiber laser using a nonlinear amplifying loop mirror. It delivers a 7.81 MHz train of pulses with an average power of 213 mW, corresponding to pulse energy higher than 27 nJ. The output chirped pulses can be recompressed down to ∼114fs with a grating pair compressor. The nonlinear phase shifts accumulated in the long fiber cavity can be used to compensate for the mismatched third order dispersion and increase the compressed pulse quality. The laser shows excellent stability and environmental robustness during the test.**

***Index Terms*—Dissipative solitons, mode-locked fiber laser, nonlinear amplifying loop mirror.**

I. Introduction

ALL-NORMAL dispersion (ANDi) mode-locked fiber lasers have received extensive attention in recent years and are considered as promising alternatives to traditional bulk solid-state ultrafast lasers such as Kerr lens mode-locked Ti:sapphire lasers. Pulses in the ANDi fiber laser are highly positive chirped and can be recompressed to ultrashort duration outside the cavity. The boundary condition of the cavity is satisfied by the dissipative process, in which the pulse duration and chirp are reduced by a spectral filter. An important feature of the ANDi laser is that it can be easily scaled to high pulse energy several orders of magnitude larger than that of a typical soliton laser [1]. Chong *et al.* reported on an ANDi laser delivering stable pulses with 26nJ energy that can be dechirped to 165 fs duration [2]. By combining a short single-mode fiber (SMF) and a long section of polarization-maintaining (PM) fiber, Kharenko designed an all-fiber Yb oscillator that can generate ∼20nJ, ∼200 fs pulses [3]. With a similar scheme, the pulse energy can scale up to 50nJ by optimizing the cavity length and using double-clad large-mode-area fiber [4].

Although fiber lasers are generally considered to be adjustment-free and environmentally stable, the robustness and reliability are related to the specific cavity structure and the mode-locking mechanism used. A large number of fiber lasers, including all of the lasers mentioned above, utilize free-space components or non-PM fibers to favor nonlinear polarization evolution mode-locking. Such lasers are sensitive to environmental perturbations, as mechanical stress and temperature or humidity changes can induce random birefringence in non-PM fibers and change the laser performance. As a result, this kind of laser cannot be widely used beyond the laboratory in practice. Therefore, it is of great value to study how to improve the output pulse energy from femtosecond mode-locked fiber laser without sacrificing the environmental robustness of the cavity design. The use of PM fibers can significantly increase the robustness against environmental perturbations. Using cross-splicing technology, mode-locking based on NPE has been successfully demonstrated in all-PM-fiber cavities [5]–[7]. However, the output pulse energy is relatively low. Real saturable absorbers, such as carbon nanotubes [8], [9], semiconductor saturable absorber mirrors [10], [11], and graphene [12], [13], can also be used to build mode-locked all-PM fiber lasers. However, they suffer from a relatively low damage threshold and a tendency to degrade over time [14].

Nonlinear optical loop mirror (NOLM) and nonlinear amplifying loop mirror (NALM) are two promising mode-locking mechanisms that can be applied in all-PM configurations. Laser based on NOLM uses a fiber coupler with a coupling ratio significantly differing from 50:50. The difference in nonlinear phase shift between the two counter-propagating pulses in NOLM depends on the split ratio of the coupler and the length of the passive fiber in the loop. PIELACH *et al.* reported on an ultrafast all-PM Fiber Laser based on NOLM delivering pulses of high energy of 12 nJ which can be compressed down to 250fs [15]. NALM is modified by adding a second amplifying stage inside the NOLM loop and a 50:50 coupler can be used. The second amplifier in the NALM loop allows better control of the output parameters

Manuscript received February 15, 2022; revised March 5, 2022; accepted March 10, 2022. Date of publication March 16, 2022; date of current version March 31, 2022. This work was supported in part by the National Natural Science Foundation of China under Grant 62005299. *(Corresponding author: Zebiao Gan.)*

Luqi Guo is with the State Key Laboratory of High Field Laser Physics, Shanghai Institute of Optics and Fine Mechanics, Chinese Academy of Sciences, Shanghai 201800, China, with the University of Chinese Academy of Sciences, Beijing 100049, China, and also with the ShanghaiTech University, Shanghai 201210, China (e-mail: guolq@shanghaitech.edu.cn).

Zebiao Gan and Xiaoyan Liang are with the State Key Laboratory of High Field Laser Physics, Shanghai Institute of Optics and Fine Mechanics, Chinese Academy of Sciences, Shanghai 201800, China (e-mail: gzb@siom.ac.cn; liangxy@siom.ac.cn).

Digital Object Identifier 10.1109/JPHOT.2022.3159536

and easier mode-locking operation. When the NALM loop is operated in transmission, the ends of the PM fibers used for the NALM can be connected to form the so-called "Fig. 8" laser. Lasers based on Fig. 8 configuration can deliver ultra-short pulses with a low-repetition rate but high energy in favor of applications like micromachining and biological imaging. One way to increase the single pulse energy is to increase the cavity length and reduce the repetition rate. Erkintalo *et al.* reported on an environmentally stable all-PM all-fiber giant chirp oscillator delivering 16nJ pulses that could be de-chirped to 370fs [16]. It is also possible to improve the output parameters by optimizing the structure of the laser cavity. By optimizing the repetition rate, a 6-MHz all-PM fiber oscillator delivering 10nJ pulses with 31nm spectral bandwidth which can be compressed to 93fs was demonstrated [17]. Deng *et al.* optimized the position of gain fiber in the NALM loop and achieved a 22nJ pulse output that can be compressed to 195 fs [18]. However, there is no detail about the long-term power stability of the output laser. It may also increase difficulty in reaching the stable mode-locked regime when the length difference of the passive fibers between each side of active fiber in the NALM loop becomes too small. In this paper, we demonstrate the single pulse energy scaling ability of an all-PM NALM fiber laser without sacrificing the environmental robustness. Gain fibers and passive fibers with large mode areas are used and the optical cavity has been specially designed for such lasing operation allowing the achievement of a record in term of energy /compressed pulse duration. The output pulse energy and average power are 27nJ and 213 mW respectively. The pulse duration can be recompressed down to 114fs. To the best of our knowledge, this is the highest output from an all-PM fiber oscillator mode-locked by NALM in the sub 200fs regime. We also show for the first time that the accumulated nonlinear phase shifts accumulated in the long fiber cavity can be used to partly compensate for the mismatched third-order dispersion (TOD) and improve the quality of the compressed pulses.

II. Experimental Setup and Results

The laser resonator is built in a typical fight-8 configuration as illustrated in Fig. 1. The main loop of the laser contains a 125cm long single-clad large mode area ytterbium-doped (Yb-doped) PM fiber (Nufern PLMA-YSF-10/125). The active fiber is pumped by a single-mode 980nm laser diode (Pump1) through a wavelength division multiplexer (WDM). The 10:90 fiber coupler extracts 90% of the intracavity power as output. A band-pass filter centered at 1030 nm with a 6 nm @ 0.5 dB bandwidth is used to ensure the cavity's boundary conditions. A long segment of PM single-mode fiber (SMF, ∼10m) is inserted after the Yb-doped fiber. An isolator ensures the unidirectional operation of the main loop and blocks the light reflected by NALM loop. The NALM loop is connected to the main loop by a 50:50 coupler. A 54 cm long Yb-doped fiber of the same type as the main loop is used in the NALM, which is pumped by a second single-mode 980nm fiber coupled diode (Pump2). The nonlinear phase shift accumulated in the NALM is related to the geometrical asymmetry of the loop as well as the pump direction. The length difference of passive fiber on both sides of

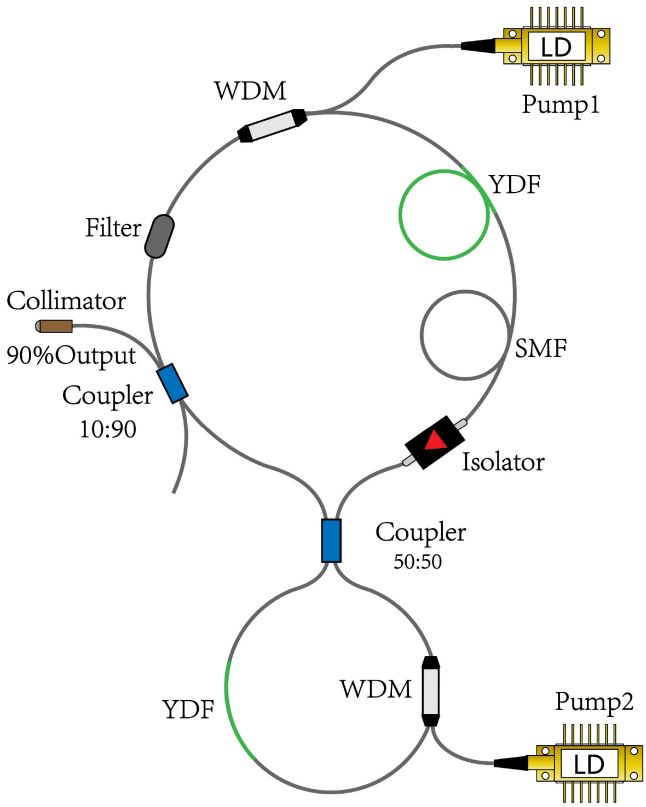

Fig. 1. Schematic diagram of the laser setup. YDF: ytterbium-doped fiber; SMF: single mode fiber; WDM: wavelength division multiplexer; LD: laser diode.

gain fiber is set to be 2m in NALM. The passive optical fibers in the laser cavity are all Nufern PM 1060L and the overall cavity length is about 26m.

The self-starting mode-locked state can be achieved by increasing the pump power of the main loop and the NALM loop to 573 mW and 519 mW respectively. In this regime, there were two pulses coexisting per round trip in the laser cavity. The single pulse mode-locking operation can be obtained by keeping the pump power in the main loop at 573mW while decreasing the pump power in NALM to 386mW. The pulse trains generated from the fiber oscillator were measured by a 4 GHz oscilloscope (KEYSIGHT DSOS404A) together with a 4 GHz photodetector (EOT ET3000), as shown in the inset (a) of Fig. 2. The radio-frequency (RF) spectrum was measured with 10Hz resolution bandwidth and 6KHz span by the same photodetector connected to an RF spectrum analyzer (Tektronix RSA607A). The fundamental repetition rate of the pulse train is measured to be 7.81 MHz, matching well with the ∼26m cavity length and the measured pulse spacing of 128ns. The signal-to-noise ratio (SNR) of the fundamental RF spectrum is over 80dB. The harmonic RF spectra were measured at a revolution of 100Hz with a span of 300MHz (inset (b) of Fig. 2). The RF trace drops smoothly without noticeable variations, confirming the high temporal stability of the single pulse mode-locking.

To further confirm that only one pulse is circulating in the oscillator, we measured the temporal characteristics of the

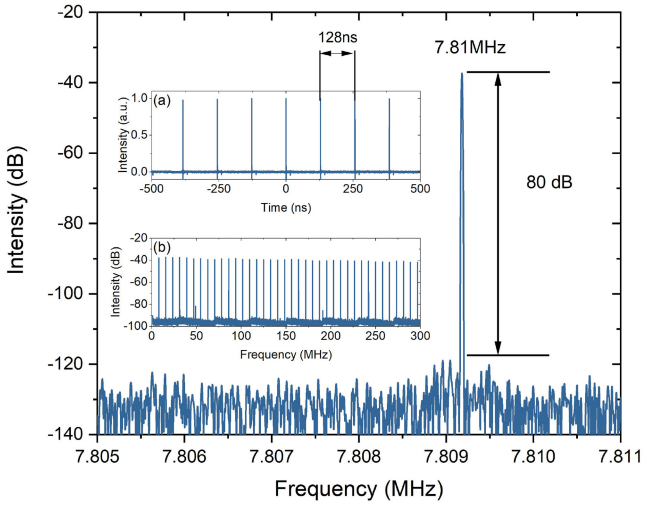

Fig. 2. RF spectrum recorded at the fundamental frequency. Inset (a): The pulse train generated from the fiber oscillator; Inset (b): Harmonic RF spectrum.

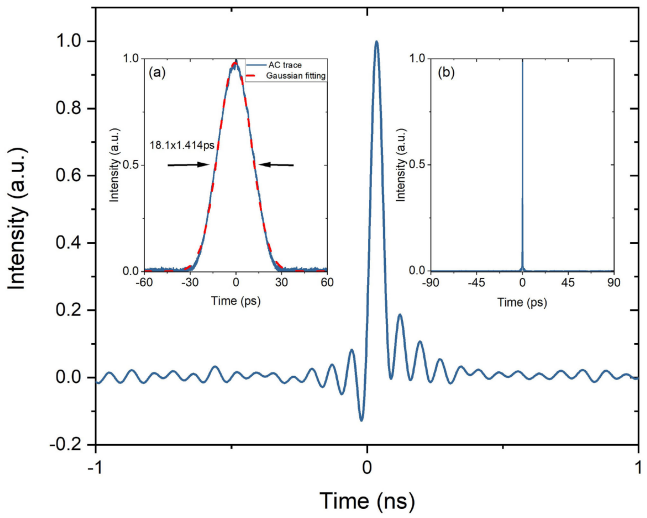

Fig. 3. Temporal wavefront of the output pulse measured by a 22 GHz photodetector and a 13 GHz bandwidth oscilloscope. Inset (a): Autocorrelation trace of the chirped output pulse; Inset (b): Autocorrelator trace of the compressed pulse with a 180ps long scanning range.

laser output at different time scales. First, a high-speed 22GHz photodetector (EOT ET-3600) and a 13GHz bandwidth oscilloscope (Keysight DSA91304A) were used to monitor the temporal wavefront. The pulse duration at full width at half-maximum (FWHM) is measured to be ∼48ps. This measurement verifies that only one pulse exists in the time interval of 50ps to 128ns. The ripple on both sides of the main pulse is due to the ringing of the photodetector, which cannot represent a multi-pulse generation. Limiting by the detector bandwidth, the oscilloscope trace cannot accurately represent the optical envelope. Assuming a Gaussian shape, the actual duration of the output chirped pulse is measured to be 18.1ps by an intensity autocorrelator (Femtochrome FR-103XL) as shown in the inset (a) of Fig. 3. Second, we compressed the chirped output pulse by a pair of transmission gratings ((LightSmyth T-1000-1040-3212-94)) and measured the autocorrelation trace in the long scanning

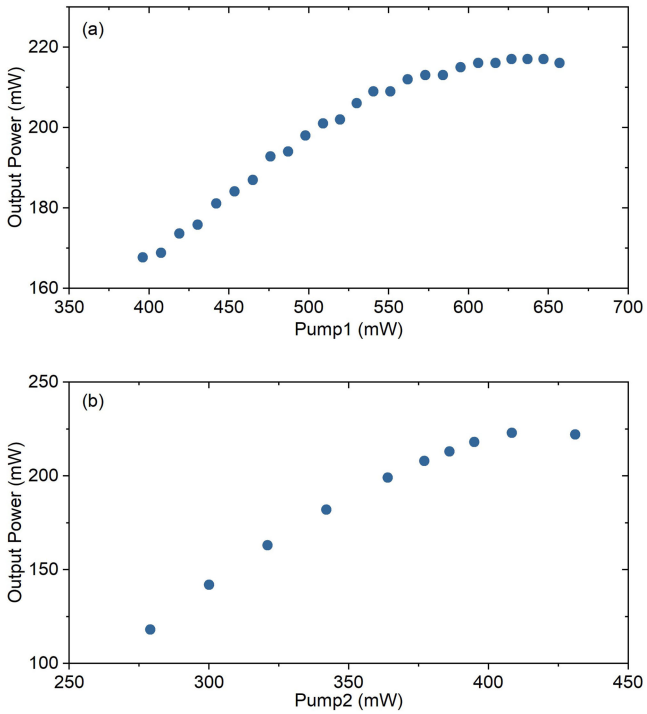

Fig. 4. Experimentally measured laser output power with respect to pump power. (a) NALM loop pump power was kept at 386mW and the main loop pump power varies from 396mW to 657mW; (b) Main loop pump power was kept at 573mW and the NALM pump power varies from 279mW to 431mW.

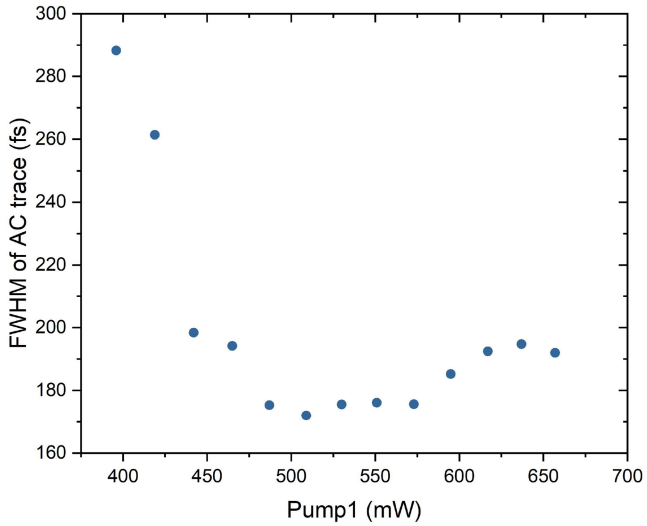

Fig. 5. The FWHM duration of the Autocorrelation trace as a function of the main loop pump power.

range as shown in the inset (b) of Fig. 3. This measurement checks out there are no satellite pulses on the shorter time scale (fs to 180ps) and the laser does not work in a noise-like regime.

When the pump power in the NALM loop was kept at 386mW, the laser can maintain a stable single-pulse mode-locked state as the main loop pump power varies from 396mW to 657mW. On the other hand, if the main loop pump power was fixed at 573mW, the NALM pump power can be adjusted between 279mW and 431mW without destroying the fundamental mode-locking state.

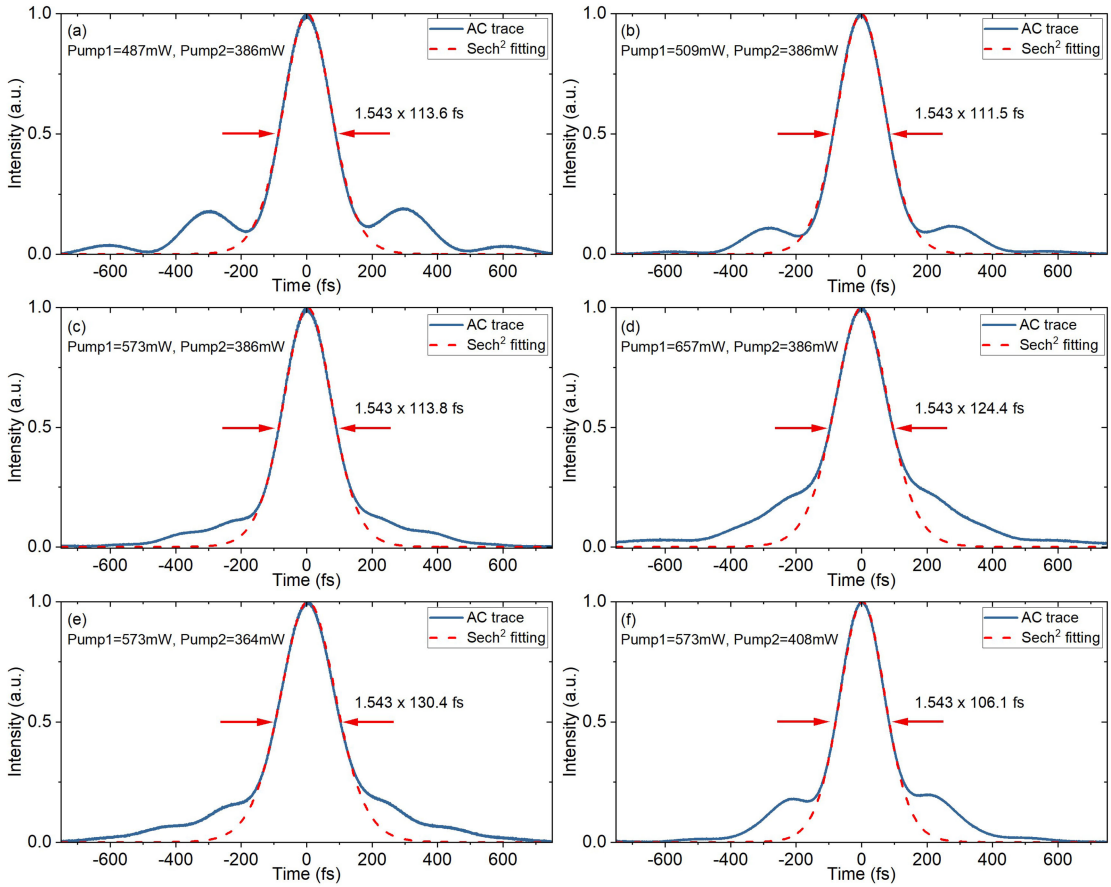

Fig. 6. Measured autocorrelation traces and fitting traces of the compressed output pulses under different pump power levels. AC: autocorrelation.

Fig. 4. shows the laser output power as a function of pump power. In both cases, the output power increases as the pump power increases and gradually saturates. The measured laser average power can be higher than 220mW, corresponding to pulse energy larger than 28nJ. Further increase of pump power will cause the laser to lose its fundamental mode-locked state.

The output chirped pulses were recompressed by a grating pair with 1000 lines/mm and the compressor was used at a Littrow angle. The grating spacing was independently optimized for minimal autocorrelation width (FWHM) under different main loop pump power when the NALM loop pump power was fixed at 386mW. As shown in Fig. 5, the FWHM duration of the autocorrelation trace first decreases with the increase of the pump and then remains at around 175fs. With the further increase of the pump power, the pulse width increases again.

The measured autocorrelation traces of the compressed pulses under different main loop pump power are presented in more detail in Fig. 6(a) to (d). As shown in these figures, the duration and quality of compressed pulse significantly depend on the main loop pump power. Pulses circulating in the oscillator with a ~26m fiber length will accumulate a large amount of dispersion. Although the second order dispersion can be eliminated by the grating pair compressor, the TOD will add and cannot be compensated simultaneously. The mismatched TOD leads to incompressible sidelobes in the autocorrelation trace at low pump power as shown in Fig. 6(a). However, when the main loop pump power increased to 509mW, the large sidelobes are decreased as shown in Fig. 6(b). Although there is still a small wing structure in the autocorrelation trace due to residual TOD, a relatively clean pulse is obtained when the main loop pump power is increased to 573mW as shown in Fig. 6(c). The FWHM duration of the autocorrelation trace is measured to be 175.6fs and the corresponding compressed pulse duration is estimated to be 113.8fs with a convolution factor of 1.543 assuming a sech^2 pulse profile. The reason that the pulse quality increases as the main loop pump power increases is due to the accumulated nonlinear phase shifts which can be used to compensate for the mismatched TOD. This technique is commonly used in the so call nonlinear chirped pulse amplification. With the main loop pump power further scaling up, the mismatch between the nonlinear phase shifts and the TOD increases and lead to the pedestals of de-chirped pulses becoming more obvious as shown in Fig. 6(d). In Fig. 6(c), (e), and (f), the main loop pump power is kept at 573mW while the NALM loop pump power is varied. We can observe a similar relationship between the compressed pulse quality and the NALM loop pump power. These results indicate that it doesn't matter where the nonlinear phase shifts are accumulated in the oscillator, the quality of the compressed pulses mainly depends on the total amount of nonlinear phase accumulation. It should be noted that once the pump powers were fixed, the measured autocorrelation traces of the compressed pulses were stable and the pulse shapes did not fluctuate.

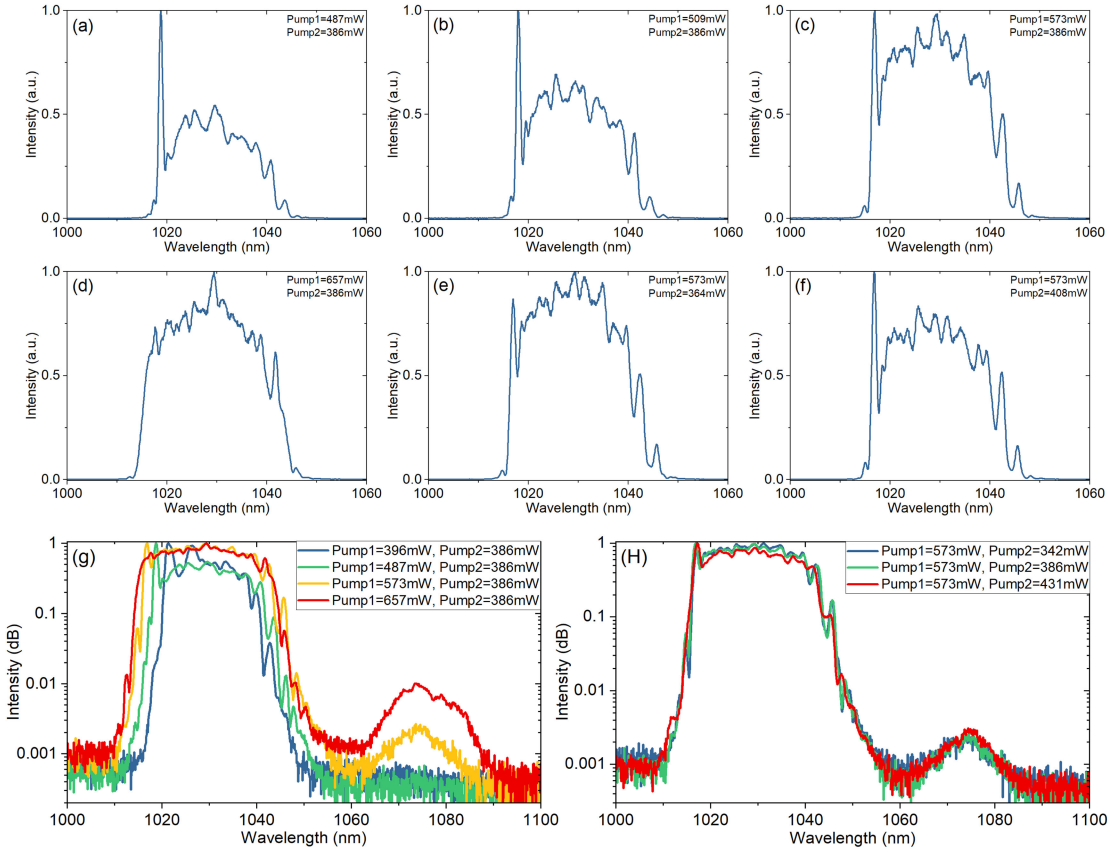

Fig. 7. Spectral characteristics of the laser output under different pump power levers. (a)∼(f): in linear scale; (g)∼(H): in logarithmic scale.

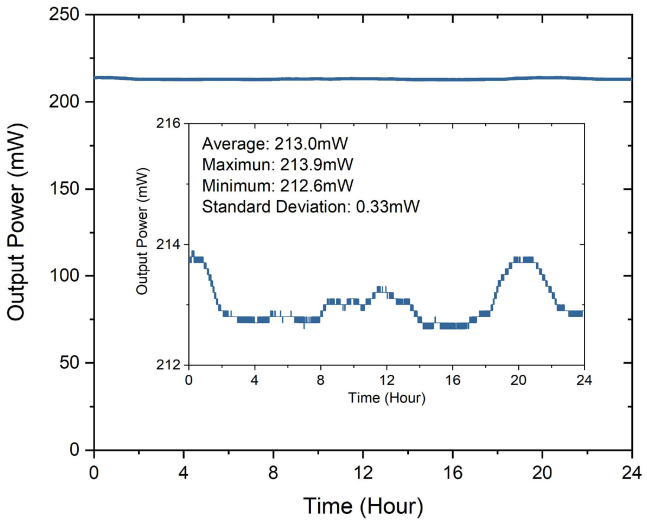

Fig. 8. Output power stability test in 24 hours.

Fig. 7 (a) and (f) show the laser output spectrum measured with an optical spectrum analyzer (YOKOGAWA AQ6370D) under different pump power levels. The spectrums have steep edges which is the typical characteristic for the ANDi lasers [19], [20]. The uneven modulation in the spectrum is due to the effect of self-phase modulation, high order dispersion, and the spectral filtering induced by NALM. For each case, the spectrum is centered near 1030nm and has a board width above 20nm. Fig. 7(g) and (h) present the spectrum in logarithmic scale. The spectral width gradually broadens along with the strengthening of the first-order stimulated Raman scattering (SRS) signal when the main loop pump power increases. The SRS signal at around 1075 nm becomes obvious when the main loop pump power reaches 657mW, which is the maximum output of the laser diode (Pump1). However, the Raman emission is still 20 dB below the laser emission and the integrated Raman signal counts only about 0.6% of power in total laser emission. In contrast, adjusting the pump power in the NALM loop does not significantly change the intensity of the Raman signal. Note that in the main loop, there is a long PM passive fiber after the gain fiber, so it is easy to excite the SRS signal when the pulse peak power is high. In the NALM, the input pulse is divided into two equal waves counter-propagating in the loop and the fiber length in the NALM is relatively short. After the NALM, a large amount of laser power is extracted out of the cavity by the output coupler. Therefore, increasing the pump power in the NALM loop will not significantly enhance the Raman signal.

To demonstrate the stability of the laser, the output power was measured over 24 hours by a power meter (Ophir 12A). The pump power in the main loop and the NALM loop was set to be 573mW and 386mW respectively. The average output power is 213.0mW. The coefficient of variation (standard deviation divided by average) and peak-valley fluctuation (The difference between the maximum and minimum divided by the average) is

only 0.15% and 0.61% respectively in 24 hours. These results verify the excellent stability of the mode-locked all-PM fiber laser with environmental robustness.

III. Conclusion

In conclusion, we have demonstrated pulse energy and average power scalability of an environmentally stable mode-locked all-PM fiber laser using NALM. The self-starting laser can deliver a 7.81MHz train of pulses with an average power of 213mW, corresponding to pulse energy higher than 27nJ. The output chirped pulses can be recompressed down to ∼114fs by a pair of gratings. To the best of our knowledge, this is the highest output from an all-PM fiber oscillator mode-locked by NALM in the sub 200fs regime. As the nonlinear phase shifts accumulated in the long fiber cavity can be used to compensate for the mismatched third order dispersion, we can optimize the pulse quality of the compressed pulses by adjusting the pump power levels. Note that the nonlinear phase shift accumulated in each fiber segment depends on both the pulse peak power and the fiber length. Therefore, it is also possible to optimize the total nonlinear phase accumulation by carefully designing the distribution of fiber segments in the mode-locked fiber laser cavity without changing the laser output power. The laser shows excellent stability and environmental robustness. We measured the laser output power over 24 hours, the coefficient of variation and peak-valley fluctuation is only 0.15% and 0.61% respectively.

References

[1] F. W. Wise, A. Chong, and W. H. Renninger, "High-energy femtosecond fiber lasers based on pulse propagation at normal dispersion," *Laser Photon. Rev.*, vol. 2, no. 1-2, pp. 58–73, Apr. 2008.

[2] A. Chong, W. H. Renninger, and F. W. Wise, "All-normal-dispersion femtosecond fiber laser with pulse energy above 20 nJ," *Opt. Lett.*, vol. 32, no. 16, pp. 2408–2410, Aug. 2007.

[3] D. S. Kharenko, E. V. Podivilov, A. A. Apolonski, and S. A. Babin, "20 nJ 200 fs all-fiber highly chirped dissipative soliton oscillator," *Opt. Lett.*, vol. 37, no. 19, pp. 4104–4106, Oct. 2012.

[4] D. S. Kharenko, V. A. Gonta, and S. A. Babin, "50 nJ 250 fs all-fibre Raman-free dissipative soliton oscillator," *Laser Phys. Lett.*, vol. 13, no. 2, Feb. 2016, Art. no. 025107.

[5] J. Szczepanek, T. M. Kardas, C. Radzewicz, and Y. Stepanenko, "Ultrafast laser mode-locked using nonlinear polarization evolution in polarization maintaining fibers," *Opt. Lett.*, vol. 42, no. 3, pp. 575–578, Feb. 2017.

[6] J. Szczepanek, T. M. Kardas, C. Radzewicz, and Y. Stepanenko, "Nonlinear polarization evolution of ultrashort pulses in polarization maintaining fibers," *Opt. Exp.,* vol. 26, no. 10, pp. 13590–13604, May 2018.

[7] W. Zhang *et al.*, "Ultrafast PM fiber ring laser mode-locked by nonlinear polarization evolution with short NPE section segments," *Opt. Exp.*, vol. 26, no. 7, pp. 7934–7941, 2018.

[8] K. Kieu and M. Mansuripur, "Femtosecond laser pulse generation with a fiber taper embedded in carbon nanotube/polymer composite," *Opt. Lett.*, vol. 32, no. 15, pp. 2242–2244, 2007.

[9] Y.-W. Song, S. Yamashita, C. S. Goh, and S. Y. Set, "Carbon nanotube mode lockers with enhanced nonlinearity via evanescent field interaction in D-shaped fibers," *Opt. Lett.*, vol. 32, no. 2, pp. 148–150, Jan. 2007.

[10] U. Keller *et al.*, "Semiconductor saturable absorber mirrors (SESAM's) for femtosecond to nanosecond pulse generation in solid-state lasers," *IEEE J. Sel. Topics Quantum Electron.,* vol. 2, no. 3, pp. 435–453, Sep. 1996.

[11] O. Okhotnikov, A. Grudinin, and M. Pessa, "Ultra-fast fibre laser systems based on SESAM technology: New horizons and applications," *New J. Phys.,* vol. 6, Nov. 2004, Art. no. 177.

[12] D. Popa, Z. Sun, F. Torrisi, T. Hasan, F. Wang, and A. C. Ferrari, "Sub 200 fs pulse generation from a graphene mode-locked fiber laser," *Appl. Phys. Lett.*, vol. 97, no. 20, Nov. 2010, Art. no. 203106.

[13] J. Xu, J. Liu, S. Wu, Q.-H. Yang, and P. Wang, "Graphene oxide mode-locked femtosecond erbium-doped fiber lasers," *Opt. Exp.*, vol. 20, no. 14, pp. 15474–15480, 2012.

[14] P. Mouchel, M. Kemel, G. Semaan, M. Salhi, M. L. Flohic, and F. Sanchez, "Limitations of graphene nanocoated optical tapers for high-power nonlinear applications," *Opt. Mater. X*, vol. 1, 2018, Art. no. 100003.

[15] M. Pielach, B. Piechal, J. Szczepanek, P. Kabacinski, and Y. Stepanenko, "12 nJ, 250 fs pulses from an all-PM-fiber laser oscillator," in *Proc. Conf. Fiber Lasers XVIII - Technol. Syst., Electr. Netw.*, 2021, Art. no. 11665.

[16] M. Erkintalo, C. Aguergaray, A. Runge, and N. G. R. Broderick, "Environmentally stable all-PM all-fiber giant chirp oscillator," *Opt. Exp.*, vol. 20, no. 20, pp. 22669–22674, Sep. 2012.

[17] Y. Yu *et al.*, "Highly-stable mode-locked PM Yb-fiber laser with 10 nJ in 93-fs at 6 MHz using NALM," *Opt. Exp.*, vol. 26, no. 8, pp. 10428–10434, Apr. 2018.

[18] D. Deng, H. Zhang, Q. Gong, L. He, D. Li, and M. Gong, "Energy scalability of the dissipative soliton in an all-normal-dispersion fiber laser with nonlinear amplifying loop mirror," *Opt. Laser Technol.*, vol. 125, May 2020, Art. no. 106010.

[19] A. Chong, J. Buckley, W. Renninger, and F. Wise, "All-normal-dispersion femtosecond fiber laser," *Opt. Exp.*, vol. 14, no. 21, pp. 10095–10100, Oct. 2006.

[20] A. Chong, W. H. Renninger, and F. W. Wise, "Properties of normal-dispersion femtosecond fiber lasers," *J. Opt. Soc. Amer. B-Opt. Phys.*, vol. 25, no. 2, pp. 140–148, Feb. 2008.